



Automated Lesion Detection-Based Symptome Mapping In Patients With Sensory Deficits

Laboratoire de Recherche en Neuroimagerie - LREN
Département des neurosciences cliniques
Centre Hospitalier Universitaire Vaudois (CHUV)

Fabian Hilti

Supervisor: Prof. B. Draganski

Co-supervisor: F. Kherif

January 12, 2013

Table of contents		Page
1	Introduction	3
1.1	Anatomical basics	3
1.2	The cerebrovascular Incident	5
1.3	Function-lesion studies	6
1.4	Neuroimaging techniques	8
1.5	Lesion detection	10
1.5.1	Previous work on lesion detection methods	12
1.5.2	Previous methods in function-lesion studies	13
2	Methods	14
2.1	Data processing	14
2.2	Lesion detection	17
2.3	Statistical analysis	18
3	Sample description	18
4	Results	19
4.1	The design matrix	19
4.2	The lesion overlap map	20
4.3	Grey matter analysis	21
4.4	White matter analysis	23
4.5	Lesion-based analysis	24
5	Discussion	25
6	Conclusion	26
	References	27

1. Introduction

The human brain is the most complex structure known. With its high number of cells, number of connections and number of pathways it is the source of every thought in the world. It consumes 25% of our oxygen and suffers very fast from a disruption of its supply. An acute event, like a stroke, results in rapid dysfunction referable to the affected area. A few minutes without oxygen and neuronal cells die and subsequently degenerate. Changes in the brains incoming blood flow alternate the anatomy and physiology of the brain. All stroke events leave behind a brain tissue lesion. To rapidly react and improve the prediction of outcome in stroke patients, accurate lesion detection and reliable lesion-based function correlation would be very helpful. With a number of neuroimaging and clinical data of cerebral injured patients this study aims to investigate correlations of structural lesion locations with sensory functions.

1.1 Anatomical basics

This section is a brief introduction based on different sources. The following informations could be found in any anatomical standard work and is therefore with only few references. Brain and spinal cord form the central nervous system (CNS). Subdivisions of the brain are the telencephalon, the cerebellum, the diencephalon, and the brainstem. The telencephalon consists of the two areas the cerebral cortex and the basal ganglia. The higher human encephalization quotient (relative brain size) compared to other mammal species relies on the expansion of the cerebral cortex. This is the largest part of the brain, with a surface area of about 2200 cm. The widely enlarged frontal lobe is responsible for higher abilities such as abstract thinking and planning, reasoning and self-control. The part of the cerebral cortex for vision is also enlarged. The cortex is divided into four "lobes", the frontal, parietal, temporal and occipital lobe.

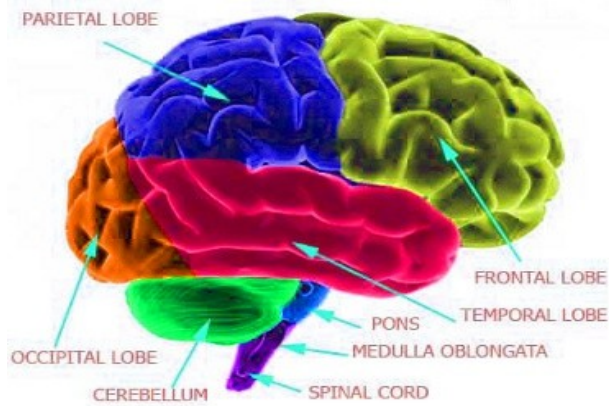


Figure 1: The lobes of the cerebral cortex with brainstem and cerebellum¹.

Neurons and unmyelinated fibers build up the cerebral cortex and give it a grey color, to which the name grey matter (GM) refers. Below a large amount of axons connect the cerebral cortex to other brain regions, which are heavily myelinated and appear white, which has led to its anatomical description as white matter (WM).

The basal ganglia have indirect connections with the cerebral cortex and is involved in motor control. The cerebellum is located posterior and inferior of the telencephalon and contains about 50% of the neurons found in the CNS. It has a large number of input connections, e.g. visual input and auditory input. The diencephalon consists of the thalamus, the subthalamus, and the hypothalamus, which are structures involved in memory, hormone releasing, and regulation of the body temperature and appetite. The brainstem, located directly posterior of the spinal cord, receives sensory information input and sends out motor signals through cranial nerves.

Brain and spinal cord are surrounded by cerebro spinal fluid (CSF), which is clear fluid, acting as "cussion", that protects the brain mechanically and immunologically. CSF is formed in the plexus choroideus and in other locations and is absorbed by venous blood. Every day around 500 ml of CSF is produced and turns over about four times a day, since the brain contain only around 150 ml. The rest is drained into circulation.

The two brain hemispheres, connected through the corpus callosum, resemble each other structurally but are functionally different. The left hemisphere includes the language center and processes information in a logical and sequential manner. In a more intuitively and randomly way, on the right hemisphere interpreting of visual information and spatial processing take place. The right part of the body is controled by the left hemisphere and vice versa. The different brain lobes have different tasks. The frontal lobe provides higher functions like interpreting touch, vision and sounds. And in the posterior part of the frontal lobe we find the motor cortex, which controls movement. In the temporal lobe there are centers for language understanding, the memory process and audition. Whereas the parietal

lobe interpretes language, tactile sensations as well as pain and temperature. In the occipital lobe visual information is processed.

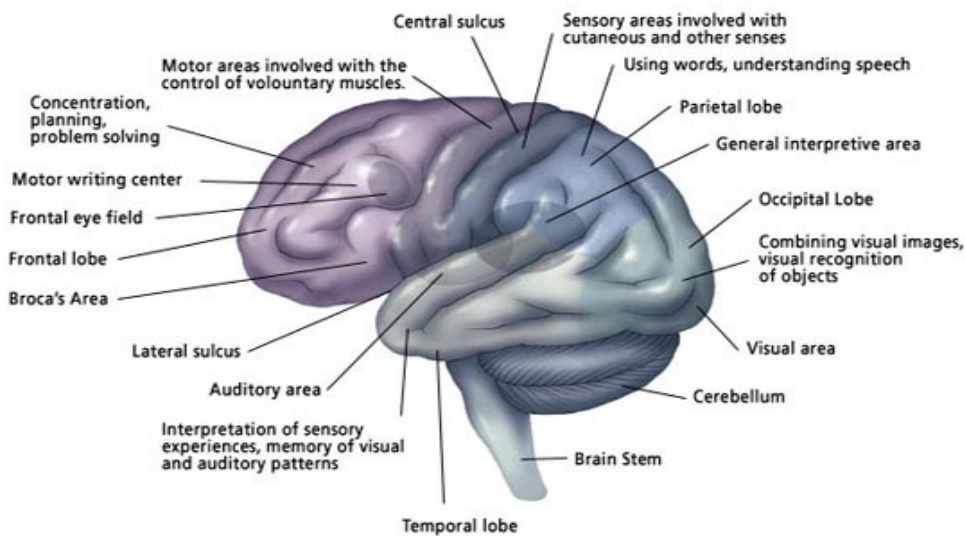


Figure 2: Some motor, sensory and association areas of the cerebral cortex ².

1.2 The cerebrovascular incident

With 11% worldwide cerebrovascular accidents (CVA) are the 2nd most frequent cause for human death in the last 20 years. And a huge part of all severe long-term disabilities result from such events ³⁴. Commonly known as stroke, there is an interruption of blood supply and a part of brain cells undergo a sudden death. This could be a block of vessels by a blood clot (ischemic stroke, in around 85% of CVAs) or the rupture of a blood vessel, causing blood to leak out into the brain (hemorrhagic stroke, 15% of CVAs). The resulting lack of blood flow and oxygen supply, or the compression due to increased pressure resulting from a bloodmass may cause permanent neurological damage or even death ^{4 5 6}.

Initially the stroke lesion is classified as an acute lesion, which eventually could be seen as a slight change in image intensity in an MRI. Hyperacute strokes could not be seen in FLAIR or T1 images.

The central irreversibly infarcted tissue is also known as an ischemic core. These dead neurons are surrounded by a peripheral region (the ischemic penumbra) composed of cells that are ceased to function, but yet they are still viables and potentially salvageables ^{7 8}. Later, the tissue becomes necrotic and is cleaned out by scavenger cells, leaving behind a void which is subsequently filled with CSF. Then the lesion is classified as necrotic or chronic.



Figure 3: Chronic stroke lesion stage ⁹.

Different symptoms may occur consequently, e.g. weakness or paralysis of an arm (motor cortex affected), vision changes (visual cortex affected) or difficulty in speaking or understanding of words (language center affected). Some stroke patients will not have any symptoms at all.

Treatment should be induced within three hours from the onset to ensure optimal chances of recovery. Immediate treatment may be drugs that break up blood clots, if the patient has suffered an ischemic stroke, or an urgent surgery to remove a pool of blood and repair damaged blood vessels in case of a hemorrhagic stroke. In our times strokes tend to increase because of factors like lifestyle and ageing of the population ¹⁰. Brains plasticity offers an opportunity to recover from strokes. Cortical functions and neuronal circuits can be reorganised. These rehabilitation is supported by training and particular treatments. About 10% of all stroke patients regain all functionality and about 50% of all stroke patients are able to leave the hospital with some medical assistance.

1.3 Function-lesion studies

In function-lesion studies, or lesion-based function determination, the science community tries to complete the brainmap of tasks. Therefore correlations and dependencies between clinical disabilities and radiologically (including MRI) existing lesions are statistically analysed.

Some of the recent findings of this research domain are presented here in order to introduce our goal, which is to use automated lesion detection to find lesions (mainly strokes) that affect the perception of sensory information. Sensomotoric disabilities after brain injuries are very common but anyway not very often studied.

By the means of lesion mapping techniques, there has for example been shown relationship

between superior temporal and premotor areas with biological motion perception in a work by Saygin et al.¹¹. Whereas Noskin et al. could for example show that dexterity and grip strength are independent from each other and are controlled by different entities¹². Further, in 2010, it has been shown by Lo et al. that motor functions of the hand depends on the integrity of the corticospinal pathway. They also found critical anatomical areas of converging premotor and motor projections that, in the case they are damaged, have a negative influence on the recovery potential¹³.

In terms of language performance and other cognitive tasks a bit more work have been done in the past years. Piras et al., in a lesion mapping study of 2009, analysed the different brain regions implicated in number and word reading¹⁴. Or, related to this, it has been shown that four Brodmann areas were involved in word reading¹⁵. Important regions for semantically correct speech have been found in the left inferior frontal gyrus and anterior temporal lobe¹⁶. Borovsky et al., 2007, conducted the first voxel-based lesion analysis of speech production performance in aphasic patients¹⁷, and Leff et al., in 2009, could show the influence of the auditory short-term memory on spoken language comprehension ability¹⁸. That a comprehensive method to categorize brain regions according to their function and predicting the outcome of cerebrally injured patients could be feasible has been shown by Skidmore et al., 2007¹⁹. Another study has focused on the particular outcome and recovery of language after stroke and with a variety of language measures it yielded a range of probable recovery patterns and the first data-led system²⁰.

In a long term projection, the scientific research around this study also should possibly provide a recovery model for predicting functional outcomes and survival after stroke. This is a challenging task due to the huge variability of individual impairment evolution and the not yet known magnitude of influence by certain prognostic factors²¹. In this study the focus is on the sensory dysfunction and statistically highlights the areas that in case of a cerebral lesion are most likely responsible for a sensory dysfunction.

But before this could happen, we need the images to analyse. That is why the next section coarsely introduces neuroimaging and the magnetic resonance imaging technique, respectively.

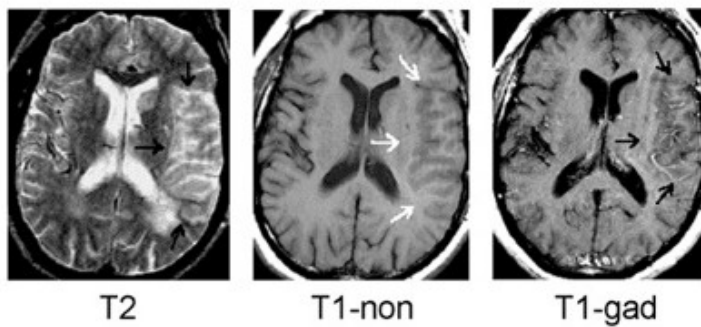
1.4 Neuroimaging techniques

The technique needed is magnetic resonance imaging (MRI), which provides an insight of the brain. Computed tomography (CT), the older and radioactive variant of neuroimaging, is less helpful, due to less spatial image resolution and its ethical incompatibility with the acquisition of data of healthy controls.

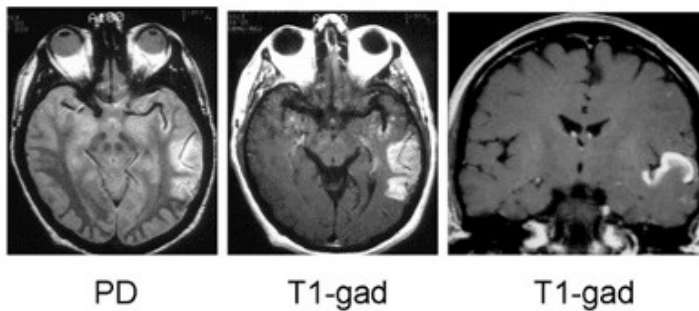
MRI is the technique to align nuclear spins by the means of magnetic fields making them absorb and emit electromagnetic energy that could be detected. The tissue specific signals have different modalities which could be visualized independently offering a large number of information. These modalities present an important instrument in the everyday clinical practise as well as in the domain of medical research. Recent advancement (high image resolution, good signal-to-noise ratio and nice contrast of tissues and water contents) increase detection accuracy and the evaluation of the affected brain region after an undergone stroke. In the different modalities there is moreover apriori knowledge about the time evolution of the lesion extension included.

The most conventional magnetic resonance representations are the T1- and T2-weighted images, which are able to show for example anatomical inconsistencies with different sensitivity to vascular lesions. In a MRI-investigation different tissues show up with different image intensities. T1-weighted (T1w) images are the standard basic scans and the most clinically used. They separate fat from water (the water shows up darker and the fat brighter) and therefore, they provide an optimal contrast between the white matter (WM), the grey matter (GM) and the cerebrospinal fluid (CSF). In an acute stroke, the intensity of a fresh lesion in the T1w scans is the same as the intensity of the GM, while for the chronic stage, it has the intensity of CSF or is replaced by CSF, respectively. T1w images are particularly usefull in showing older lesion.

MRI of Acute Stroke



MRI of Subacute Stroke



MRI of Chronic Stroke: 2 Cases

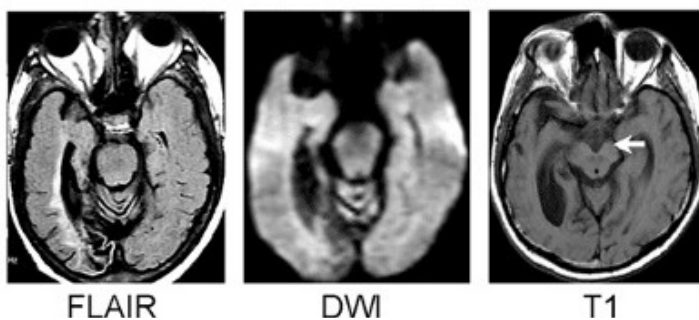


Figure 4: Examples of different MRI modalities on different stroke states ²².

In a T2 weighted (T2w) MRI, CSF instead shows up bright white and WM shows up in a darker image intensity. GM is represented by a grey color, similar to that in a T1w MRI. T1w and T2w Images are not useful in detecting acute ischemic brain injuries, whereas diffusion- (DWI) and perfusion-weighted imaging (PWI) have more ability to do so. These techniques were able to visualize movement in the fluid brain compartment. Disadvantages of DWI and PWI are a poor spatial resolution and a lack of grey to white matter contrast. Diffusion weighted imaging (DWI) does focus on the micromovements of the water molecules inside the voxels, what leads to useful information about the surrounding structure of these molecules. The single voxel intensity in the image refers to a single maximal measurement of the rate of water at that location. Injured tissue represents an area of restricted diffusion and on DWI it appears brighter, whereas intact brain tissue is darker relatively. This sequence is much more sensitive than a T1w to early changes after stroke, but it works only within a short time window of about three weeks and is brightest in average after seven days ²³. DWI,

therefore, is a powerful instrument to handle hyper-acute stroke. Furthermore brain fluids have the tendency to follow major fibre tracts. This can be visualized by DW-scans and is called tractography.

After being able to visualize a lesion on MRI the next step will be to handle this data and extract the information needed and finally delineate it and separate it as good as possible from the intact structure. That is where we come to the chapter of segmentation and lesion tracking.

1.5 Lesion detection

Knowing the position of the infarction is certainly crucial. This leads to the demand for a accurate lesion detection method. Therefore a separation into WM, GM and CSF is helpful. Segmenting the brain into different tissue classes can be based on image intensity, color, or texture. The voxels inside one segmented region are similar in some way. The two main methods to use when segmenting the brain are either manually or automatically. Both techniques have their pros and cons. There is also a combination of the two methods available where the brain is first automatically segmented and then some post-processing is performed by an operator.

For a long time manual segmentation was the standard technique for lesion identification ²⁴. Within every 2D slice of the MRI scan, lesions were identified by a trained expert and were mouse-based outlined or filled. The operator has to have a 3D imagination of the structures to ensure continuous tissue classes in a 2D images- based delineation process. This former gold-standard has the big disadvantage of being influenced by inter- and intra- observer errors and of consuming extremely much time ²⁵. Especially in large data sets a time requirement of several days to even weeks for the correct delineation of one scan renders a daily clinical application impossible.

For a potential fully automatic detection method of cerebral lesions we need to go into Computational Anatomy (CA), a growing discipline to quantitatively analyse the variability of objects and organisms. CA could as well be applied to analyse features of the human brain. Using Voxel-Based Morphometry (VBM) region-wise volumetric comparisons among populations of subjects are possible ²⁶. In a generative model individual subject images can be warped to a template to reach intersubject registration. This includes the informations about the deformation field.

Automated voxel-based lesion detection methods of the whole brain provide a sensitive estimation of intact and damaged tissue by assigning a continuous signal intensity value to each voxel. The Statistical Parametric Mapping software package SPM²⁷, running under MATLAB (from The MathWorks, inc.) has a flexible framework to accommodate tools for automated lesion detection. Originally the SPM freeware is devised for statistical parametric mapping and processing of raw PET or fMRI data into standardised stereotactic space for then undergoing voxel-based statistics. So the gold-standard or state-of-the-art software of choice for this study is the latest version of SPM8. SPM refers to the construction and assessment of spatially extended statistical processes used to test hypotheses about functional imaging data²⁷.

The automated segmentation is based on a prior probability of finding specific tissue at specific brain areas that most likely are grey matter (GM), white matter (WM) and cerebrospinal fluid (CSF). The probability itself comes from the information of normal brains (forming a standard space) combined with likelihood estimations of observing the corresponding intensity value. Therefore, automated segmentation approaches critically depend on successful pre-processing of the data. Pre-processing commonly involves normalization to standard space, segmentation of the images to the three tissue classes GM, WM and CSF, and finally smoothing with a Gaussian kernel²⁸. The original segmentation routine of SPM8 has classified brain tissue only in these three classes, which already causes problems in segmenting out bone tissue for example. And the templates were based on normal healthy brains only. Consequently segmentation of abnormal brains gives incorrect results. Further it is only a mono-spectral implementation which can be improved by making it multi-spectral by including the information of, for example, other MRI modalities like T2 weighted images or DWI. So far segmentation into the different tissue classes via an automated mechanism is fast and does provide acceptable results, only in the case the patient's brain anatomy is without lesions or other aberrations. This could be for example older brains with significant losses of brain mass or cortical thickness.

But the original segmentation routine within SPM is permanently undergoing improvements like the segmentation routine add-ons of Mohamed Seghier²⁵. This is discussed more extensively in the next section.

1. 5. 1 Previous work on lesion detection methods

Automated lesion delineation in pathological cases is thus a clinical demand and therefore an active research field. It has been studied in multiple sclerosis, tumors, and ischemic brain lesions. But the performance of the automated detection remains largely unsatisfying. For stroke detection Shen et al. have explored using voxel intensity variations and tissue distribution probability within predefined maps for tissue types^{29 30}. This is done by a version of a fuzzy c-means algorithm that, after tissue type identification for all voxels, does a comparison with standard tissue probability maps (TPMs) to detect outliers. As this method is based on voxels intensity and location, it could miss some of the outliers, whose signal intensity is similar to the one of the expected tissue. Like, for example, in the case of fresh lesions located in high-probability GM regions.

The introduction of an additional tissue type in Mohamed Seghiers Automated Lesion Identification (ALI) has much improved the original segmentation routine of SPM8. The assumption of this is that each lesion comprises voxels with abnormal signal intensities that could be seen as an additional tissue class besides GM, WM and CSF²⁵. The purpose of ALI is to minimise misclassification of abnormal tissue into GM and WM portions by segmenting them out as CSF or if possible into a fourth extra tissue class. This atypical tissue class represents a mean between the priors of WM and CSF and better results could be achieved by iteratively running the segmentation procedure. Finally outliers were detected by an algorithm already introduced in one of his previous publications³¹. This approach has a better robustness compared to Shen's but lesion detection accuracy measure is below the fulfilment of quality (with a reported Dice's coefficient of only 0.64).

In another recent work touching this field, the idea is that a brain lesion can be seen as an abnormality in the four brain features the tissue homogeneity, the tissue composition, the shape and the lateral deviation³². After a spatial normalisation and a segmentation of an image without any tissue priors, for each feature an "abnormality map" is generated, whose combination will give the locations and the extension of the damaged brain area. But maps have to be combined manually to ensure an accurate representation of the lesion. Therefore, this method is not fully automated. The research group supporting this work recently also has developed an outlier-detection framework based on the combination of three image features that can be extracted from a damaged brains T1w image: the intensity, the possible change in the folding structure and the thickness of the lesion with respect to the healthy part of the brain³³. The resulted outlier finding is used as a lesion prior in the module 'New Segment' of SPM8 and therefrom the healthy part of the three main brain classes (GM, WM and CSF) are derived. This is discussed in more detail in chapter 2.1.1.

Thanks to such improvements the user now can identify abnormal/lesioned brain tissue and generate lesion overlap maps (LOMs) of groups or populations. In LOMs voxels that are frequently lesioned in a certain population can be identified, which could be very helpful for lesion-symptom mapping.

Lesion-symptom correlation studies with various methods already have been done before and a brief excursion to some of them is given in the next section.

1. 5. 2 Previous methods in function-lesion studies

To conduct function-lesion mapping studies precise lesion identification is essential.

Generally, the gold-standard method is still the manual definition of abnormal brain tissue by a trained professional^{34 35}. But this method is laborious, time-consuming and operator-dependent³⁶. Subsequently semi-automated and fully automated procedures for lesion delineation have been proposed.

In the ROI approach a patients' cohort is defined on the basis of lesions in a particular brain region (region of interest – ROI) and then tested for behavioural differences from a healthy control population. On the other hand the opposite approach focused on the behavioural deficit and subsequently created a frequency map of the lesions to find a responsible common area. But Bates et al., 2003, stated that such a categorization failed because of too coarse description of the lesion and behavioural performance³⁴. The ROI approach further has the limitation of the predefined lesion location that renders impossible to find not yet known relationships over the whole brain.

A widespread semiautomated technique is the so called Voxel-based Lesion-Symptom Mapping (VLSM) representing a voxel-by-voxel analysis of manually delineated brain lesions³⁴. It has for example been used to identify specific anatomical regions for maintaining motor performance after a stroke event. VLSM statistically assesses effects of the lesions on behavioural scores on a voxel-by-voxel basis and yields high resolution statistical maps, rather than a large region of interest or lesion categories as described before. But as a semiautomated technique it depends on observer input and is therefore susceptible to problems of subjectivity and reproducibility.

This study aims at clarifying relationships between a brain lesions extent/localisation and a particular (dys)function. And it focuses on potential regions in the whole brain related to sensitivity impairment. To address this question, magnetic resonance (MR) images of 54 patients with brain lesions, mainly stroke, has been used and automated lesion detection followed by whole brain voxel-based statistical analysis have been conducted.

2. Methods

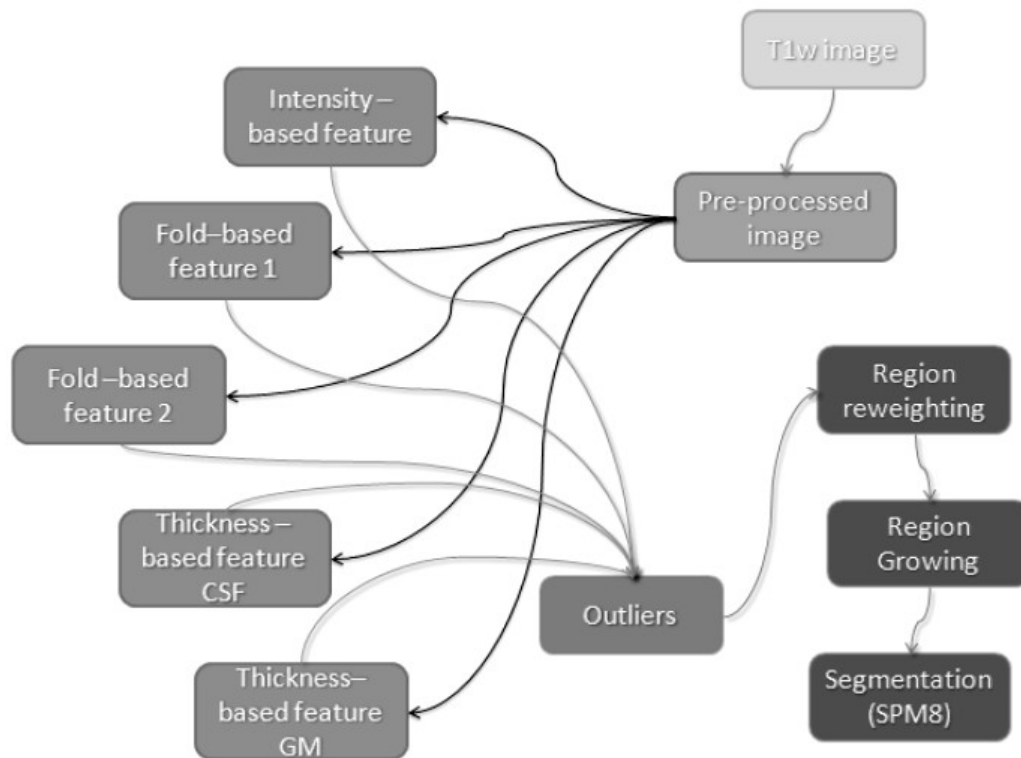


Figure 5: Schematic representation of the main steps of the procedure ³⁸.

2.1 Data processing

The first step of the pre-processing part is to normalize the T1w images into the standard MNI space and then perform a bias-correction and a skull stripping. Therefor the model of a canonical brain is needed whereafter all diffeomorphic brains could be warped. Within the computational framework Statistical Parametric Mapping (SPM) algorithms like the Diffeomorphic Anatomical Registration Through Exponential Lie Algebra (DARTEL) enable smooth and continuous mapping between corresponding points of 2 images. The relative shapes of the images are then encoded in the parameters of the mapping. The software combines segmentation, bias correction and spatial normalisation through the inversion of a single unified model ²⁴. The unified model combines tissue classification, intensity bias and non-linear warping in one probabilistic model. The image intensities are modelled as a mixture of Gaussians (MOG), and a prior probability that the tissue classes are defined by certain voxel intensities. The priors for the tissue classes are encoded in deformable TPMs.

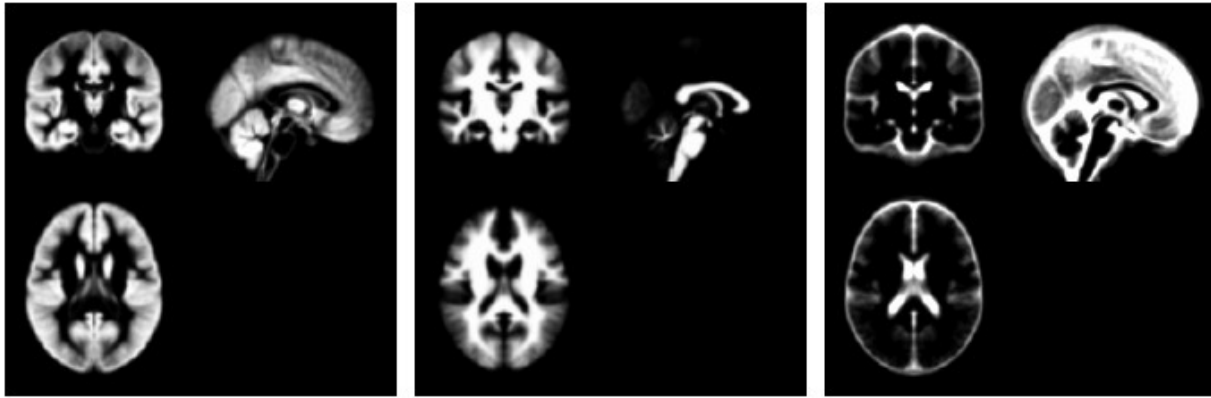


Figure 6: Tissue probability maps for GM (left), WM and CSF (right). Image intensity values range from zero (black) to one (white). A higher value represents a higher probability of the voxel belonging to the the corresponding tissue.

The tissue classification process requires the image volumes to be registered to the TPMs. Which assigns to the different parts of the image prior probabilities of belonging to one of the different considered tissue classes. These priors are then combined, by the means of Bayes rule, with the probabilities for different tissue classes derived from different voxel intensities to give a posterior probability. The circularity-problem of this procedure, since the registration requires an initial tissue classification and vice versa is tried to come by, by combining both components into a single generative model. That includes parameters that account for image intensity non-uniformity. Estimating the model parameters (for maximum a posteriori solution) involves alternating among classification, bias correction and registration steps. This approach provides better results than simple serial applications of each component.

The TPMs include the probabilities of finding a tissue class at a certain location combined with a estimated likelihood of the observed intensity values, and they were made by taking a large amount of normal brains. They are modified versions of the maps of the ICBM Tissue Probabilistic Atlases and are kindly provided by the International Consortium for Brain Mapping ³⁷. The original data are derived from 452 T1-weighted scans, which were aligned with an atlas space, corrected for scan inhomogeneities, and classified into GM, WM and CSF. These data were then affine registered to the MNI space and down-sampled to 2mm resolution.

Researchers around this study recently have added an outlier-detection framework based on extra features extractable of the patients MRI data: the integrity of the folding structure and the thickness feature of the lesion ³³. To remove high frequencies the normalized image is smoothed with a 7mm full width at half maximum (FWHM) Gaussian kernel.

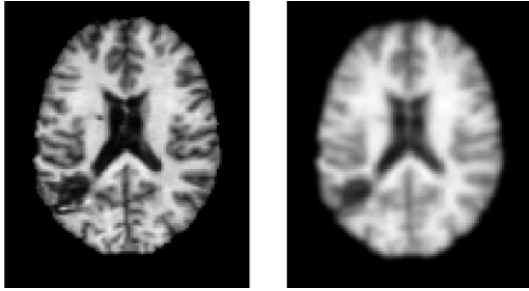


Figure 7: Image smoothed with Gaussian kernel 7mm FWHM.

The fold feature should express changes in the brains folding structure caused by a stroke and the modifications are quantified by steerable filters. A map of the brain convolutions is obtained by detecting edges and ridges separately, summing them up, and subsequently smoothing with a Gaussian kernel of 7 mm FWHM.

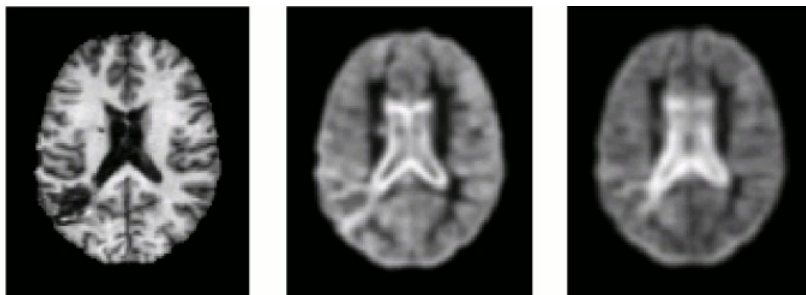


Figure 8: Illustration of the fold feature.

The third one is the thickness feature or local thickness. Lesioned parts of GM and CSF are very likely to be thicker than corresponding healthy parts. It represents per definition the largest diameter of a sphere fitting into the volume at a given point.

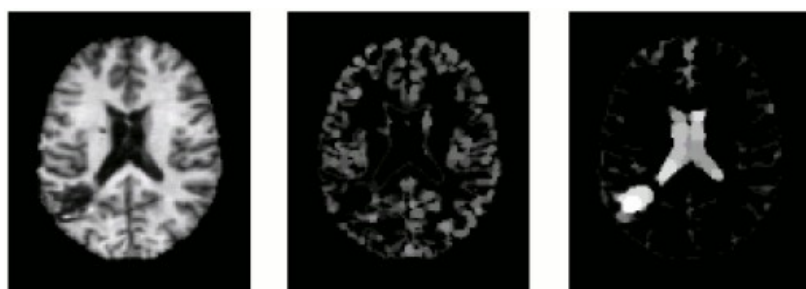


Figure 9: Illustration of the thickness feature.

2.2. Lesion detection

This three features combined give us another map. After yielding this map we have five features from which we can in the following step detect the outlier voxels. To accomplish this task the algorithm of multivariate Gaussian Mixture Model-Expectation Maximization (GMM-EM) is used ³⁸.

Before 16 control persons were taken to approximate the voxel-distribution in a healthy brain by a few centroids supposed to represent an average subject. The energy function thereby, that need to be minimized, will be the sum of the squared difference between each candidate value and the nearest reference centroid ³⁸.

Then the distribution of all features across the 16 control subjects is estimated with the multivariate GMM-EM. This adds to every point i of the image a 5-dimensional vector $f_i = [F_i, F_{fold 1}(i), F_{fold 2}(i), F_{CSF}(i), F_{GM}(i)]'$. This serves as the measure for the outlier detection. By an approximation of K Gaussians (K being the value that maximize the BIC validity criterion) we obtain the distribution of the controls set $p(f_i)$ becoming the measure for the detection. If the value for $p(f_i)$ is small the corresponding vector f_i appears only rarely in the control set and its voxel i most probably is an outlier ³⁸.

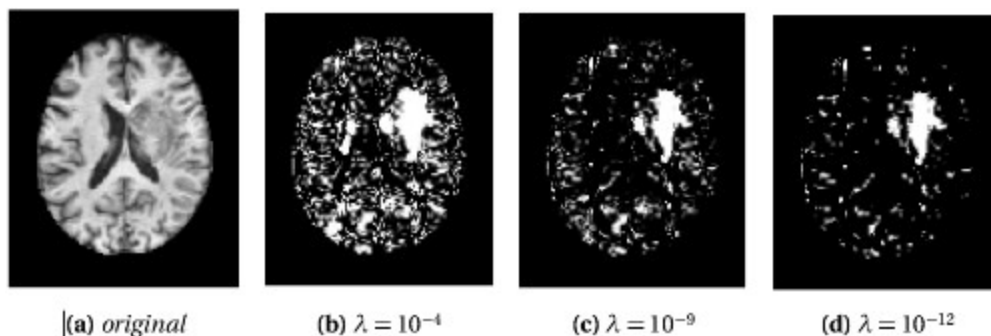


Figure 10: Lesion detection for different λ -values.

At the end there is a threshold value defined as a function depending of the mean „distance“ between the centroid population and the Gaussians multiplied by a factor λ with the role of controlling the outlier-detection sensitivity. The tuningfactor should be around 10^{-12} to „clean“ artefacts (Figure 10). The post-processing includes the use of a region reweighting algorithm to reduce noise and a region growing will refine the final outlier region and serves as prior for the final segmentation in SPM8's 'New Segment', whereupon the final probability maps are based ³⁸.

2.3 Statistical analysis

The final probability maps of each patient were overlapped to generate the lesion overlap map (LOM) (s. 4.2), indicating the number of patients who have a lesion at any given voxel. This should serve as illustration of the spatial distribution of lesions over our 54 patients.

The statistical analysis used VBM, a whole-brain, unbiased, semi-automated technique for characterizing regional differences in structural MRIs ²⁶. The analysis is performed on the smoothed GM-images using the general linear model as implemented in SPM8. Therefore all GM images were put into a multiple regression model. Non-linear and linear effects of the age of the patients have been compensated by including them as covariates. Only regressions that showed significant P-values (<0.05) after correction for multiple comparison over the entire brain are considered.

3. Sample description

From a sample of the Max-Planck Institute in Leipzig, Germany we included analyses of the structural damage from 54 patients having or not having different degrees of incapacities after an intracerebral event. The deficit mostly resulted from strokes, in 23 cases in the medial cerebral artery (MCA) on the left side, in 19 cases in the MCA on the right. In addition four subjects had an intracerebral bleeding, four neoplasia, three a traumatic event and one a colloide kyste. 16 patients are female and 38 are male. The average time between the event and the scan date was 51,5 weeks and the median timespan in between 26.6 weeks. The longest timespan between event and scan was 537 weeks and the shortest 10 weeks. So no fresh or acute lesions were included. The average age is 49 years, the median age is 46,5 years and ranges from 20 to 73 years.

The 3D datasets were acquired using a 3T whole body MR system with 12-channel RF receive head coil.

A fast acquisition of T1-w anatomical brain imaging was performed based on the 3D modified driven equilibrium Fourier transform (MDEFT) sequence (time repetition TR: 7.92 ms; echoes time TE: 2.48 ms; inversion pulse TI: 910 ms; flip angle: 16°; fat saturation; bandwidth 195 Hz/pixel; acquisition time approx. 13 min.), with an isotropic resolution of 1 mm and compensation for B1 inhomogeneities.

4. Results

4.1 The design matrix

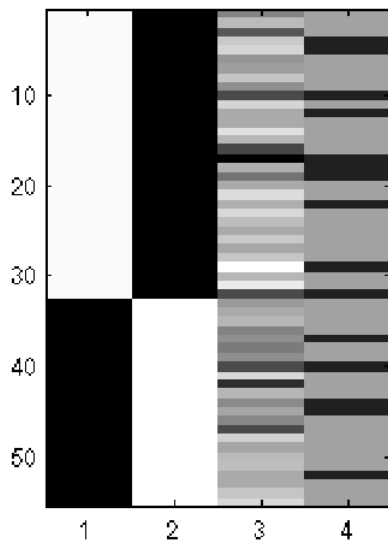


Figure 11: The design matrix used in the regression analysis. The 54 grey matter volumes were entered as the dependent variable (y-axis). The patient-specific independent variables are encoded in the columns (for each subject one value) – 3) Age, 4) Gender.

4.2 The lesion overlap map

The lesion overlap map (LOM) of the patients with intact sensory functions shows that there is less lesion overlap compared to Figure 13, what suggests that there are also smaller lesions. And independent from functional deficits lesions are mainly accumulated around the origin of the middle cerebral artery as well as slightly less accentuated in the area of the bifurcation of the posterior cerebral artery (PCA). This is slightly more expressed on the left MCA and the right PCA.

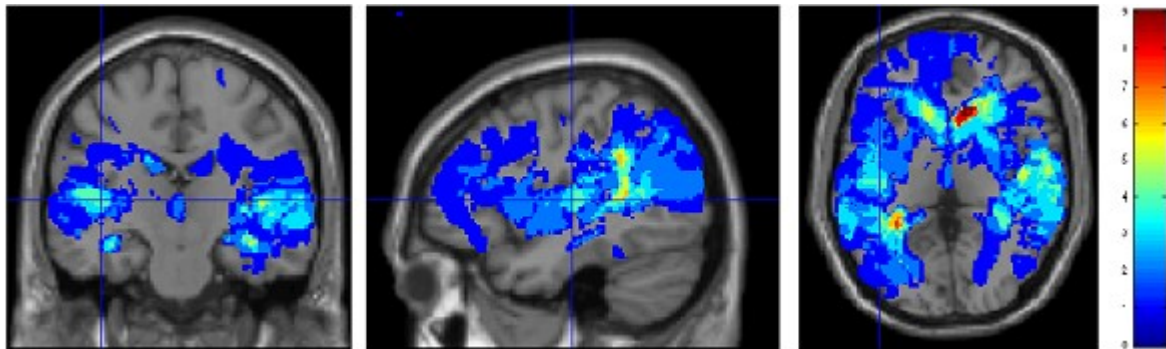


Figure 12: LOM of patients without major deficit. The amount of overlap is encoded in colors from 0 (very few overlap) to 10 (maximal overlap) .

In the LOM of the patients suffering from sensory deficits there is much more overlap and most probably more damage. The lesions in this second group concentrate in different regions. Strongest overlap is again at the origin of MCA and PCA but, in opposition to Figure 12, the lesion-overlap is stronger at right MCA and left PCA. But principally, it shows a higher involvement of deeper structures like the internal capsule, putamen, the thalamus and the insular lobe (Figure 13).

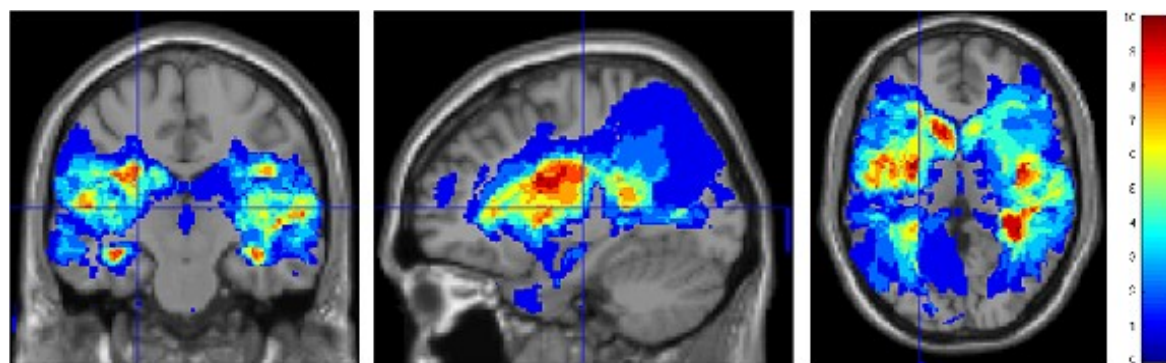


Figure 13: LOM of patients with sensory deficits. The amount of overlap is encoded in colors from 0 (very little overlap) to 10 (maximal overlap) .

4.3 Grey matter analysis

The analysis shows that if sensomotoric functions are less intact, the right temporal lobe is more often involved. Areas around the right sylvian fissure (sulcus lateralis) and the opercular region (s. Figure 14) shine up much more (s. Figure 13) than in the corresponding images where people have less symptoms (s. Figure 15), in which highlighted regions are more randomly distributed. The hippocampal territory is also involved to a higher degree (s. Discussion) as well as partially the right head of the caudate nucleus. The distribution of lacking tissue caused by damage in Figure 13 is more likely to be not by chance only, but marks certain areas with important functions for sensation (s. Discussion).

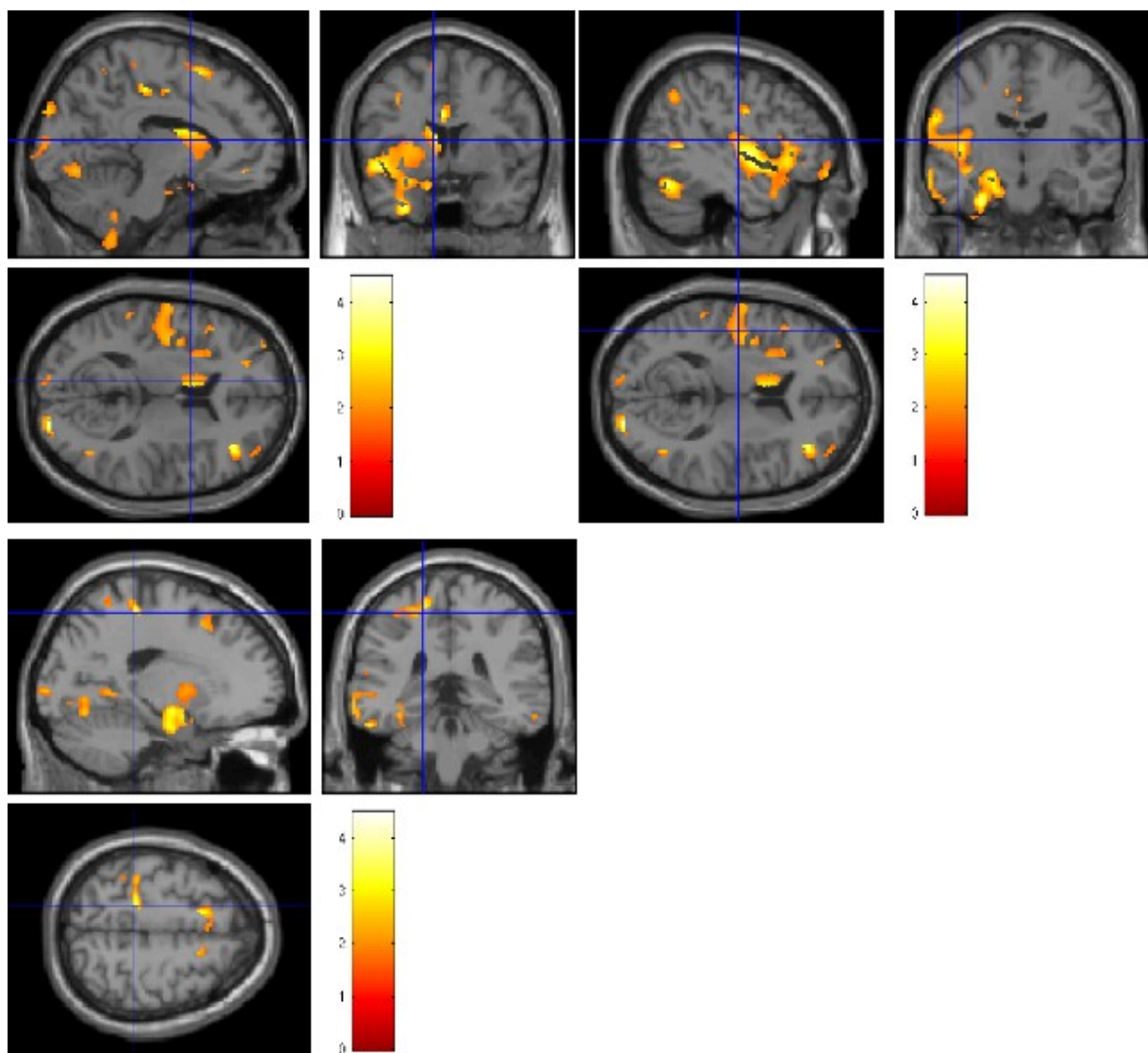


Figure 13: Illustrations of regions that are more likely to be absent due to damage in patients with a sensory deficit.

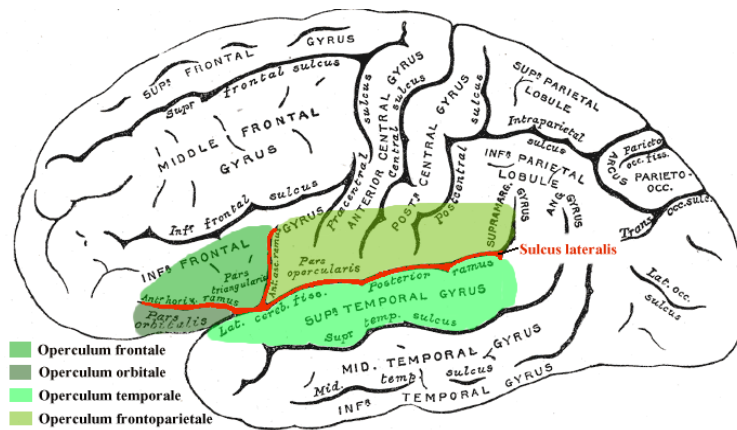


Figure 14: Illustration of the opercular region ³⁹.

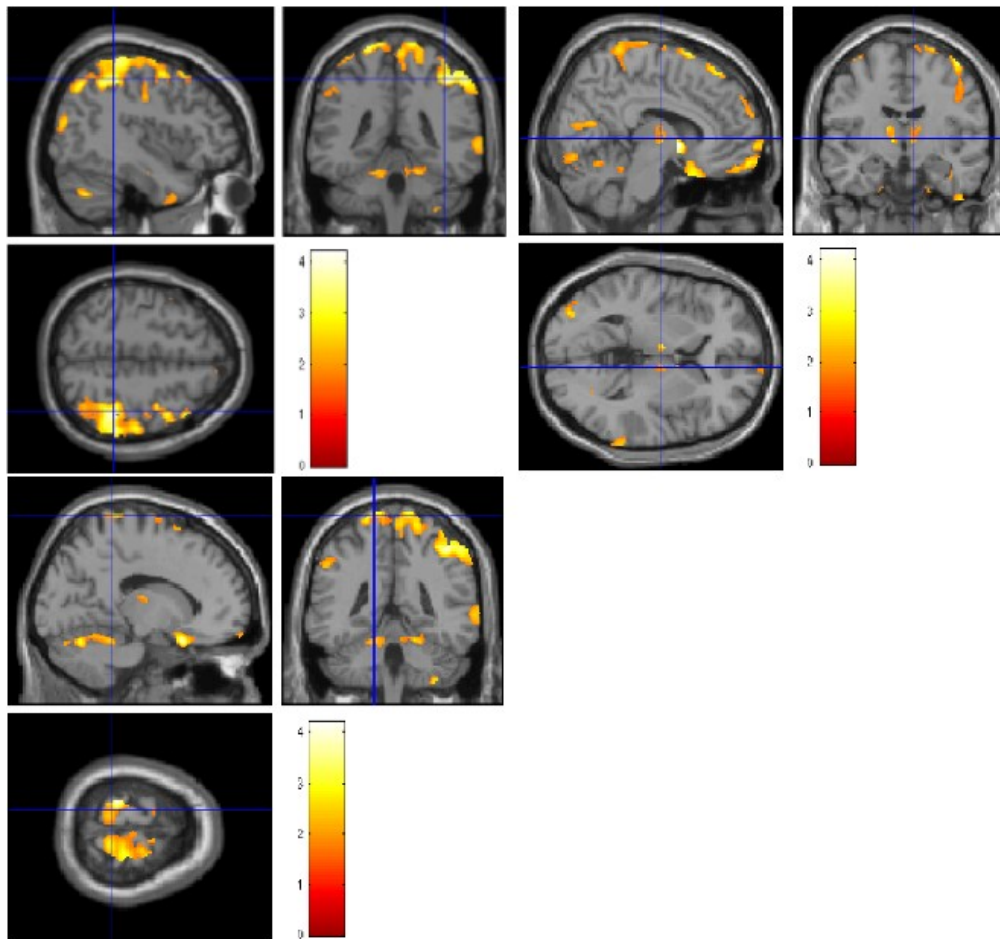


Figure 15 : This shows regions that are more often intact in patients with sensory deficits than in patients without. Typically there is no pattern recognizable. This result is unspecific and has no particular meaning because we are looking for lacking and not additional parts, but it serves as a comparison to Figure 13.

4.4. White matter analysis

Taking into account WM, the lesion, or lack of substance, regarding the occurrence of major sensory restraints, typically is located in the area of the spino-thalamico-cortical tract. In the upper right images in Figure 16, the main detected lesion in the middle is touching the whole pathway throughout the posterior limb of the internal capsule. On the upper left image of Figure 16, it seems that the lack of substance touches a big portion of the thalamus from the cranio-lateral direction. And it shows that the whole internal capsule is involved. The lower image on the left possibly suggests an involvement of the upper part of the tail of the caudate nucleus. And finally the lower right Image shows perfectly the three parts, the posterior and the anterior limb and, in the middle, the genu of the internal capsule (s. Figure 16). The detected differences in Figure 17, representing additional tissue in symptomatic patients compared to non-symptomatic do not represent any particular brain region and don't seem to be meaningful.

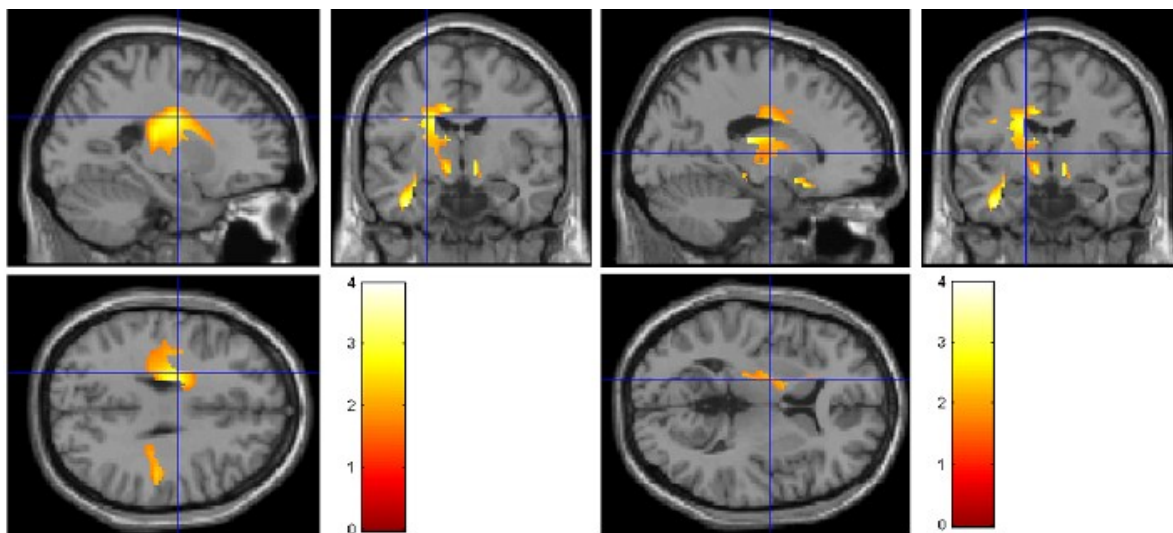


Figure 16: Illustration of the zones in the WM that are more likely damaged due to cerebral injury with consecutive sensory deficits.

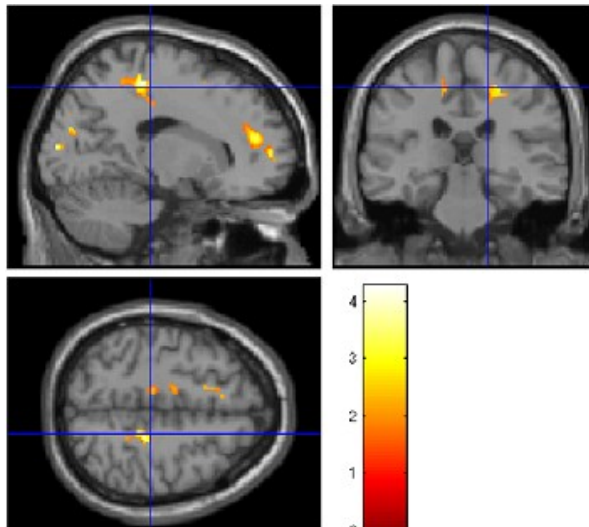


Figure 17: Illustration of the zones that contain additional tissue in cases of brain lesions compared to symptomless controls.

4.5 Lesion-based analysis

Finally our attention goes to the average lesion based on the fusion of all tissue probability maps and features, respectively, and its subtraction from the healthy control. The analysis revealed two separate lesions which both touch the right insular lobe (s. Figure 18). The lower one lays at the beginning of the sylvian fissure or the anterior insula, mainly of the temporal lobe. The second one is located at the end of the posterior limb of the internal capsule where the spino-thalamico-cortical tract fans out. It extends into the outer opercular area.

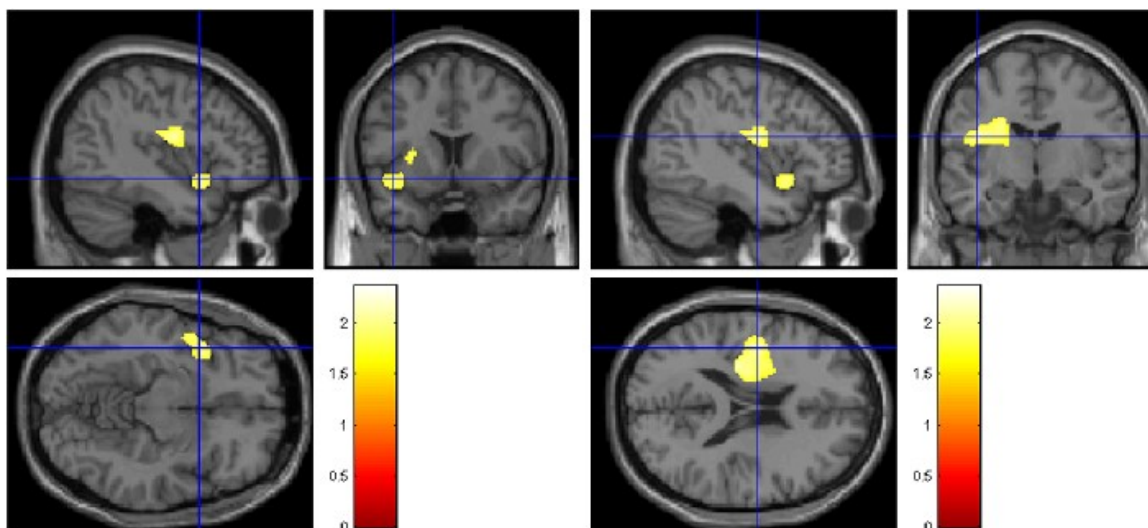


Figure 18: The lesion map showing the average lesion that has been detected in patients with sensory deficits.

5. Discussion

These results could be seen as a proof for the validity of the here applied automated segmentation procedure. But also they confirm the hypothesis of an inner opercular region as a territory involved in the treatment of wide-spectrum somatosensory information. The outer operculum contains the S2/PV sensory areas ⁴⁰ (Figure 19), which could well explain why the largest common lesion in our impaired patient contingent tends to reach into it (s. light green part in the left image in Figure 18). In our final average lesion (s. Figure 18) as well as in the GM-parts, missing in impaired patients (s. Figure 13), all sensory regions described in Figure 19 at least partially appear except for the anterior cingulate cortex, which is for affective pain recognition and sensitively irrelevant.

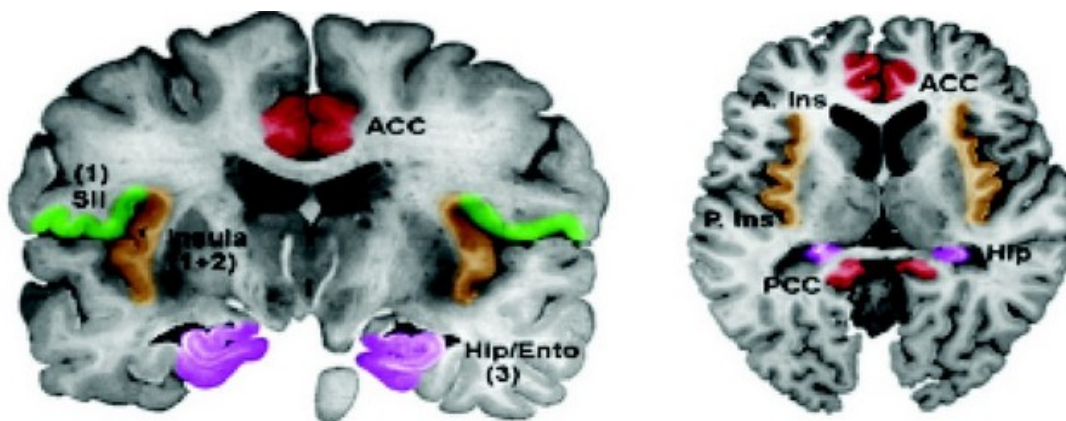


Figure 19 : Schema of pain processing related cortical areas. The highlighted areas were active in fMRI studies. Areas displayed include insula, anterior cingulate cortex (ACC), posterior cingulate cortex (PCC), primary somatosensory cortex (SI), secondary somatosensory cortex (SII), posterior and anterior insula (P. Ins and A. Ins), hippocampus (Hip), entorhinal cortex (Ento) ⁴⁰.

Looking for a primary cortex for pain sensation, the median operculum has been taken extensively under investigation in recent time. What has been found is that pain-related networks are preferentially distributed in the posterior granular insula and non-noxious thermal processing takes place in the adjacent operculum. In a review, based on over 200 publications, this cortical area that comprises the suprasylvian posterior insula and its adjoining medial operculum has been referred to as the Posterior-Insula-Medial-Operculum (PIMO) and it has been stated by the author that : “Given its particular anatomo-functional properties, thalamic connections, and tight relations with limbic and multisensory cortices, the PIMO region deserves to be considered as a third somatosensory region (S3) devoted to the processing of spinothalamic inputs .” ⁴¹As what our study concerns, we totally agree on this.

6. Conclusion

The relatively small contribution to the discourse of function-lesion mapping based on automated lesion detection of this work could be extended in plenty of ways. For example more variables could be integrated. Or one could extend the impaired-non-impaired distinction that we have chosen to a larger range of potentially informative gradations of structural damage. Better techniques to assess the patient's sensory deficit could be developed, to avoid a potentially coarse-grained estimate of the degree about a patient's sensory perception. It would be good to adopt a methodology in which both cortical damage and sensory deficit would be quantifiable in a more graded manner. This could be provided by correlating the continuous intensity value for each voxel with corresponding continuous sensory data, what would increase the sensitivity and the statistical power of the analyses. This techniques and their improvement will lead to more and more clarifications of lesion-symptom relationships.

For a long term, such research should permit to better predict the functional outcomes and survival of people affected by cerebral injury, and help to optimise the organisation of effective rehabilitation programs.

Acknowledgements

I would like to thank my supervisors Prof. Bogdan Draganski (LREN) and Ferath Kherif (LREN) and my computer science adviser Stanislaw Adaszewski (LREN) for the great help they have offered me during the development of my study. I am also grateful to Elena Najdenovska (EPFL) for providing a reliable and improved detection tool as well as methodological knowledge.

References

- 1) Brain Injury Association of America, (2013, January 12): Retrieved from: <http://www.biausa.org/living-with-brain-injury.htm>
- 2) Princeton Brain and Spine Care, Website (2012, October 29): Retrieved from: <http://www.princetonbrainandspine.com/subject.php?pn=brain-anatomy-066>
- 3) Adamson J, Beswick A, Ebrahim S. Is stroke the most common cause of disability? *Journal of Stroke and Cerebrovascular Diseases*, 13(4):171 – 177, 2004. ISSN 1052-3057.
- 4) Lopez A, Mathers C, Ezzati M, Jamison D, Murray C. Global and regional burden of disease and risk factors, 2001: systematic analysis of population health data. *The Lancet*, 367(9524):1747 – 1757, 2006. ISSN 0140-6736.
- 5) Murray C, Lopez A. Mortality by cause for eight regions of the world: Global burden of disease study. *The Lancet*, 349(9061):1269 – 1276, 1997.
- 6) Redon J, Olsen M, Cooper R, Zurriaga O, Martinez- Beneito M, Laurent S, Cifkova R, Coca A, Mancia G. Stroke mortality and trends from 1990 to 2006 in 39 countries from Europe and central Asia: implications for control of high blood pressure. *European Heart Journal*, 2011.
- 7) Bandera E, Botteri M, Minelli C, Sutton A, Abrams K, Latronico N. Cerebral blood flow threshold of ischemic penumbra and infarct core in acute ischemic stroke. *Stroke*, 37(5):1334–1339, 2006.
- 8) Srinivasan A, Goyal M, Al Azri F, Lum C. State-of-the-art imaging of acute stroke. *Radiographics* a review publication of the Radiological Society of North America Inc, 26 Suppl 1(suppl 1):S75–S95, 2006.
- 9) Naesera M et al. Brain and Language Improved picture naming in chronic aphasia after TMS to part of right Broca's area: An open-protocol study *Volume 93*, S95–105, 2005.
- 10) Warlow C, Sudlow C, Dennis M, Wardlaw J, Sandercock P. Stroke. *The Lancet*, 362(9391):1211 – 1224, 2003. ISSN 0140-6736.
- 11) Saygin A. Superior temporal and premotor brain areas necessary for biological motion perception. *Brain: a journal of neurology* 130, no. Pt 9: 2452-61, 2007,
- 12) Noskin O, Krakauer JW, Lazar R, Festa J, Handy C, O'Brien K, Marshall R. Ipsilateral motor dysfunction from unilateral stroke: implications for the functional neuroanatomy of hemiparesis. *Journal of neurology, neurosurgery, and psychiatry* 79, no. 4: 401-6, 2008 .

13) Lo R, Gitelman D, Levy R, Hulvershorn J, Parrish T. Identification of critical areas for motor function recovery in chronic stroke subjects using voxel-based lesion symptom mapping. *NeuroImage* 49, no. 1: 9-18, 2010.

Harris, R. (2010, November 22). Evaluating Internet research sources. Retrieved from <http://www.virtualsalt.com/evalu8it.htm>

14) Piras F Marangolo P. Neuropsychologia Word and number reading in the brain: Evidence from a Voxel-based Lesion-symptom Mapping study. *Neuropsychologia* 47: 1944-1953, 2009.

15) Chen R, Hillis A, Pawlak M, Herskovits E. Voxelwise Bayesian Lesion Deficit Analysis. *NeuroImage* 40, no. 4: 1633-1642, 2008.

16) Schwartz M, Kimberg D, Walker G, Faseyitan O, Brecher A, Dell G, Coslett H. Anterior temporal involvement in semantic word retrieval: voxel-based lesion-symptom mapping evidence from aphasia. *Brain*, 135(12): 3799–3814, 2012.

17) Borovsky A, Saygin A, Bates E, Dronkers N. Lesion correlates of conversational speech production deficits. *Neuropsychologia* 45: 2525-2533, 2007.

18) Leff A, Schofield T, Crinion J, Seghier M, Grogan A, Green D, Price C. The left superior temporal gyrus is a shared substrate for auditory short-term memory and speech comprehension: evidence from 210 patients with stroke. *Brain*, 132(12):3401-10, 2009.

19) Skidmore E, Rogers J, Chandler L, Jovin T, Holm M. A Precise Method for Linking Neuroanatomy to Function After Stroke: A Pilot Study. *American Journal of Physics* 14, no. 5: 12-17, 2007.

20) Price C, Seghier M, Leff A. Predicting language outcome and recovery after stroke: the PLORAS system. *Nature Publishing Group* 6, no. 4: 202-210, 2010.

21) Christian Weimar, Andreas Ziegler, Inke R. König, Hans-Christoph Diener, and . Predicting functional outcome and survival after acute ischemic stroke. *Journal of Neurology*, 249: 888–895, 2002. ISSN 0340-5354.

22) Medscape. (2013, January 9). Retrieved from: http://www.medscape.com/content/2003/00/45/28/452843/452843_fig.html

23) Thurnher M. (2013, January 9) Brain ischemia - imaging in acute stroke. the Radiology assistant. Retrieved from: <http://www.radiologyassistant.nl/en/483910a4b6f14>

24) Ashburner J, Friston K. Unified segmentation. *NeuroImage*, 26(3):839–851, 2005.

- 25) Seghier M, Ramlackhansingh A, Crinion J, Leffa A, Price C. Lesion identification using unified segmentation-normalisation models and fuzzy clustering. *NeuroImage*, 41(4-3):1253–1266, 2008.
- 26) Ashburner J, Friston K. Voxel-based morphometry--the methods. *NeuroImage* 11, no. 6 Pt 1: 805-21, 2000.
- 27) Wellcome Trust Centre for Neuroimaging in London, (2013, January 12): Retrieved from: <http://www.fil.ion.ucl.ac.uk/spm/>
- 28) Stamatakis E, Tyler L. Identifying lesions on structural brain images--validation of the method and application to neuropsychological patients. *Brain and language* 94, no. 2:167-77, 2005.
- 29) Shen S, Szameitat A, Sterr A. Detection of infarct lesions from brain mri images using inconsistency between voxel intensity and spatial location. A 3d automatic approach. *IEEE transactions on information technology in biomedicine a publication of the IEEE Engineering in Medicine and Biology Society*, 12(4):532–540, 2008.
- 30) Shen S, Szameitat A, Sterr A. An improved lesion detection approach based on similarity measurement between fuzzy intensity segmentation and spatial probability maps. *Magnetic Resonance Imaging*, 28(2):245–254, 2010.
- 31) Seghier M, Friston K, Price K. Detecting subject-specific activations using fuzzy clustering. *NeuroImage*, 36(3-3):594–605, 2007.
- 32) Wilke M, de Haan B, Juenger H, Karnath H. Manual, semi-automated, and automated delineation of chronic brain lesions: A comparison of methods. *NeuroImage*, 56(4):2038 – 2046, 2011. ISSN 1053-8119.
- 33) Burgener R. Quantitative image analysis of damaged brains: study of acute stroke. Master's thesis, EPFL, 2011.
- 34) Bates E, Wilson S, Saygin A, Dick F, Sereno M, Knight R, Dronkers N. Voxel-based lesion-symptom mapping. *Nature neuroscience* 6, no. 5: 448-50, 2003.
- 35) Dronkers N, Wilkins D, Van Valin R, Redfern B, Jaeger J. Lesion analysis of the brain areas involved in language comprehension. *Cognition* 92: 145-177, 2004.
- 36) Ashton E, Takahashi C, Berg M, Goodman A, Totterman S, Ekholm S. Accuracy and reproducibility of manual and semiautomated quantification of MS lesions by MRI. *Journal of Magnetic Resonance Imaging*, 17(3):300–308, 2003.

- 37) John C. Mazziotta and Arthur W. Toga. (2013, January 12) International Consortium for Brain Mapping. Retrieved from: http://www.loni.ucla.edu/ICBM/Downloads/Downloads_ICBMprobabilistic.shtml
- 38) Najdenovska E, Brain Lesion and Tissue Segmentation in MRI Stroke Patients: Acute and Chronic Stage, Master Project, EPFL, 2012.
- 39) Gray's Anatomy modified version of FIG. 726. (2013, January 12) Retrieved from : <http://upload.wikimedia.org/wikipedia/commons/b/b3/Operculum.png>
- 40) Borsook D et al. Neuroimaging revolutionizes therapeutic approaches to chronic pain. *Molecular Pain*, 3:25, 2007.
- 41) Garcia-Larrea L. The posterior insular – opercular region and the search of a primary cortex for pain. *Neurophysiologie Clinique/Clinical Neurophysiology*, 42(5):299-313, 2012.